Single but Stronger UO, Double but Weaker UNMe Bonds: The Tale Told by Cp_2UO and Cp_2UNR

Noémi Barros,[†,‡,§] Daniel Maynau,[⊥] Laurent Maron,*[,†] Odile Eisenstein,*[,‡] Guofu Zi,[||] and Richard A. Andersen[||]

LPCNO, CNRS-UPS-INSA, INSA Toulouse, 137 Avenue de Rangueil, 31077 Toulouse, France, Institut Charles Gerhardt, CNRS, Université Montpellier 2, cc1501, 34095 Montpellier, France, DEN/DRCP/SCPS/LCAM, CEA Valrhô, BP 17171, 30207 Bagnol-sur-Cèze Cedex, France, Laboratoire de Chimie et Physique Quantiques, CNRS, IRSAMC, Université Paul Sabatier, 118 Route de Narbonne, 31064 Toulouse Cedex 04, France, and Chemistry Department and Chemical Sciences Division of Lawrence Berkeley National Laboratory, University of California, Berkeley, California 94720

Received June 23, 2007

The free energies of reaction and the activation energies are calculated, with DFT (B3PW91) and small RECP (relativistic core potential) for uranium, for the reaction of Cp_2UNMe and Cp_2UO with MeC≡CMe and H_3Si-Cl that yields the corresponding addition products. CAS(2,7) and DFT calculations on Cp_2UO and Cp_2UNMe give similar results, which validates the use of DFT calculations in these cases. The calculated results mirror the experimental reaction of $[1,2,4\text{-}(CMe_3)_3C_5H_2]_2UNMe$ with dimethylacetylene and $[1,2,4\text{-}(CMe_3)_3C_5H_2]_2UO$ with Me_3SiCl. The net reactions are controlled by the change in free energy between the products and reactants, not by the activation energies, and therefore by the nature of the UO and UNMe bonds in the initial and final states. A NBO analysis indicates that the U−O interaction in Cp_2UO is composed of a single U−O σ bond with three lone pairs of electrons localized on oxygen, leading to a polarized U−O fragment. In contrast, the U−NMe interaction in Cp_2UNMe is composed of a σ and π component and a lone pair of electrons localized on the nitrogen, resulting in a less polarized UNMe fragment, in accord with the lower electronegativity of NMe relative to O. The strongly polarized $U^{(+)}-O^{(-)}$ bond is calculated to be about 70 kcal mol^{-1} stronger than the less polarized U═NMe bond.

Introduction

The synthesis and properties of the uranium metallocene derivatives Cp'_2UX, where Cp′ is 1,2,4-tri-*tert*-butylcyclopentadienyl and X is O or NR (R is Me, 4-MeC_6H_4, 4-(MeO)-C_6H_4, or 4-$(Me_2N)C_6H_4$), have been described.[1,2] The solid-state structures of the Lewis base adduct of the oxo derivative $Cp'_2UO(4\text{-}(Me_2N)C_6H_4N)$ and the base-free imido derivative $Cp'_2U(N\text{-}4\text{-}MeC_6H_4)$ show that these metallocenes are monomeric in the solid state. The oxo derivative is in equilibrium with the base-free metallocene in solution, and base-free Cp'_2UO was isolated and shown to be a monomer in the gas phase. In order to compare the chemical properties of the oxo and imido metallocenes, it was desirable to prepare imido derivatives in which the NR group is as sterically small as possible so that their electronic differences would be dominant. Although Cp'_2UNH could not be prepared, the NMe derivative was isolated and shown to be a monomer in the gas phase. Thus, an isoelectronic set of metallocenes that are as sterically similar as possible was available, so that their chemical and physical properties could be studied and compared.

These studies showed that the imidometallocenes, R = Me, 4-MeC_6H_4, react with benzophenone rapidly and cleanly to give the oxometallocene and Ph_2C═NR. This reaction showed that the bond dissociation enthalpy of UO was greater than that of UNR by the difference between C═O and C═NR, which has been estimated to be at least 30 kcal mol^{-1}.[3] Further, Cp'_2UNMe, but not $Cp'_2UN(4\text{-}MeC_6H_4)$, yielded isolable azacyclobutene derivatives with dimethyl- and diphenylacetylene, which are intermediates in the catalytic hydroamination of disubstituted acetylenes.[1,2,4] In contrast, the oxometallocene did not react with either of these acetylenes, but Cp'_2UO did react with an excess of Me_3SiX reagents, such as Me_3SiCl, to give $Cp'_2U(OSiMe_3)Cl$; however, the imidometallocenes did not react with Me_3SiCl.

The different reactivity pattern was suggested to result from the ground-state electronic structure of the metallocenes; namely, the double-bond resonance structure dominates the polar single-bond resonance structure in Cp'_2UNR, while the converse is true in Cp'_2UO. The reactivity difference can be justified by comparing the electron affinity of the isoelectronic fragments; the experimental gas-phase electron affinities (in electronvolts, eV) are O (1.46 eV),[5] NPh (1.45 eV),[6] NH (0.38 eV),[7] and NMe (0.022 eV).[8] The electron affinity values of O and NMe reflect the relative electronegativities of the nonmetal atoms, but substituent effects substantially change the electron affinity of the nitrene fragment.

In this article, DFT calculations on Cp_2UO and Cp_2UNMe, which are justified by multireference calculations, are reported. The calculations justify and extend the general correctness of

* Corresponding authors. E-mail: laurent.maron@irsamc.ups-tlse.fr; odile.eisenstein@univ-montp2.fr.
† LPCNO, CNRS-UPS-INSA, INSA Toulouse.
‡ Université Montpellier 2.
§ DEN/DRCP/SCPS/LCAM, CEA Valrhô.
⊥ Université Paul Sabatier.
|| University of California.

(1) Zi, G.; Jia, L.; Werkema, E. L.; Walter, M. D.; Gottfriedsen, J. P.; Andersen, R. A. *Organometallics* **2005**, *24*, 4251.
(2) Zi, G.; Blosch, L. L.; Jia, L.; Andersen R. A. *Organometallics* **2005**, *24*, 4602.
(3) Coates, G. E.; Sutton L. E. *J. Chem. Soc.* **1948**, 1187.
(4) Straub, T.; Haskel, A.; Neyroud, T. G.; Kapon, M.; Botoshansky, M.; Eisen, M. S. *Organometallics* **2001**, *20*, 5017.
(5) Blondel, C. *Phys. Scr.* **1995**, *58*, 31.
(6) Travers, M. J.; Cowles, D. C.; Clifford, E. P.; Ellison, G. B. *J. Am. Chem. Soc.* **1992**, *114*, 8699. Borden, W. T.; Gritsan, N. P.; Hadad, C. M.; Karney, W. L.; Kemnitz, C. R.; Platz, M. S. *Acc. Chem. Res.* **2000**, *33*, 765.
(7) Neumark, D. M.; Lykke, K. R.; Andersen, T.; Lineberger, W. C. *Phys. Rev. A* **1985**, *32*, 1890.

10.1021/om700628e CCC: $37.00
Publication on Web 09/01/2007

the qualitative bond model advanced above. In particular, the calculations of the potential energy surfaces for the reactions of Cp_2UO and Cp_2UNMe with various organic molecules show that kinetic barriers are relatively low and the reactions are under thermodynamic control, but steric effects play a role in manipulating the activation energies in the reactions of the imidometallocenes.

Strategy

Computational studies of compounds of the 5f-block metals are still relatively rare, and these studies are described in several recent reviews[9] and a database.[10] Calculations on the complexes of the 5f-block metal are rather challenging because of relativistic and correlation effects, involving the 5f electrons.[11] It is especially important to account for electron correlation in the case of energetically degenerate f shells, but such calculations require extensive amounts of computational time and it is necessary to model the real systems in order to reduce the number of atoms and therefore the amount of computational time.[12,13] The DFT approach is attractive because it opens the possibility of calculating large species, but the results should be handled with considerable caution since, by definition, DFT calculations cannot be used for highly multireference systems, that is, those systems that cannot be described by a single configuration, because they can lead to wrong conclusions about the electronic ground state of molecules, such as cerocene,[14] or to the heat of reaction, as in the case of the reduction of uranyl by dihydrogen.[12] However, it has been shown that the ground-state molecular geometry is not sensitive to the f-electronic state,[15] and DFT methods give optimized geometries in agreement with experiment.[12,16] Thus, DFT calculations should be validated by multireference calculations in the case of open-shell systems such as the actinide metal complexes described in this article. Although uranyl complexes have been studied by computational methods,[17] these UO_2^{2+} species are different from those described in this article; computational studies have been reported only recently on nitrene derivatives.[18]

The metallocenes used in the experimental study were $[\eta^5$-1,2,4-$(CMe_3)_3C_5H_2]_2UO$ and $[\eta^5$-1,2,4-$(CMe_3)_3C_5H_2]_2UNMe$, but in the computational studies these complexes were replaced by $(C_5H_5)_2UO$, abbreviated as Cp_2UO, and $(C_5H_5)_2UNMe$, abbreviated as Cp_2UNMe. The modeling of 1,2,4-$(CMe_3)_3C_5H_2$ by C_5H_5 has been used for the computational studies of lanthanide complexes reported earlier.[19] Substituents on the cyclopentadienyl rings certainly influence the spectroscopic properties in metallocene complexes, such as CO stretching frequencies in metallocene carbonyl compounds.[20] However, it is assumed that the relative free energies of the reactants, products, and transition states are reproduced correctly when C_5H_5 replaces the substituted cyclopentadienyl ligands; that is, the trends in the relative energies along the potential energy surface are reliable, unless steric effects dominate the electronic effects.[19]

In this article, small-core ECP calculations are performed on the uranium complexes in order to confirm that the DFT methods correctly reproduce the bond lengths and angles obtained in the experimental metallocenes. The metallocenes described in this article have a $5f^2$ electronic configuration and are spin triplets above about 50 K.[21] The triplet state, obtained at the DFT level of calculation, is confirmed by CASSCF calculations. The latter calculations also show that the triplet states do not exhibit significant multireference character and therefore justify the use of single-configuration methodology. The CASSCF calculations show that the small amount of configuration mixing is due to the occupation of nondegenerate 5f orbitals, and the electrons in these orbitals are not "chemically active electrons". Thus, the nature of the electronic configuration does not change from the reactants to the products, and therefore the CASSCF calculations are not done on the transition states and products. Test CASSCF calculations were carried out on the products of reactions of Cp_2UO with SiH_4 and H_3SiCl and for Cp_2UNMe with SiH_4. In all cases, the ground triplet state is dominated by a single configuration, which validates the use of the DFT method for the potential energy surfaces of these reactions. Geometry optimizations at the CASSCF level also yield results in agreement with the DFT calculations.

The order of presentation is (a) the enthalpy change for the reaction of Cp_2UNMe and $Ph_2C{=}O$ to give Cp_2UO and $Ph_2C{=}NMe$, (b) the potential energy surface for the reaction of Cp_2UNMe with $H_2C{=}O$ to give Cp_2UO and $H_2C{=}NMe$, and (c) the potential energy surfaces for the reactions of Cp_2UNMe and Cp_2UO with $MeC{\equiv}CMe$ and H_3SiCl. This order of presentation is adopted since the free energy changes between the reactants and products are defined by the bonding in the UO and UNMe fragments, which leads naturally to a bond model for these fragments. All of the energies are reported as free energies (ΔG) to account for the change of molecularity in the reactions, and the trends in ΔG parallel those in ΔE.

Results

Reaction of Cp_2UNMe with $R_2C{=}O$, R = Ph, H. The initial goal of the computational study is to determine the change in free energy for the irreversible experimental reaction illustrated in eq 1, where Cp is the 1,2,4-tri-*tert*-butylcyclopentadienyl

(8) Travers, M. J.; Cowles, D. C.; Clifford, E. P.; Ellison, G. B.; Engelking, P. C. *J. Chem. Phys.* **1999**, *111*, 5349.

(9) Pepper, M.; Bursten, B. E. *Chem. Rev.* **1991**, *91*, 719. Cao, X.; Dolg, M. *Coord. Chem. Rev.* **2006**, *250*, 900. Vallet, V.; Macak, P.; Wahlgren, U.; Grenthe, I. *Theor. Chem. Acc.* **2006**, *115*, 145. Kaltsoyannis, N. *Chem. Soc. Rev.* **2003**, *32*, 9. Hay, P. J. *Faraday Discuss.* **2003**, *124*, 69. Kaltsoyannis, N.; Hay, P. J.; Li, J.; Blaudeau, J.-P.; Bursten, B. E. In *The Chemistry of the Actinide and Transactinide Elements*, 3rd ed.; Morss, L. R., Edelstein, N. M., Fuger, J., Eds.; Springer: Berlin, 2006; Chapter 17.

(10) Pyykkö, P. *Relativistic Theory of Atoms and Molecules* 1915-RATM data base. Version 11.0, 2005. www.csc.fi/rtam.

(11) Pyykkö, P. *Inorg. Chim. Acta* **1987**, *139*, 989.

(12) Vallet, V.; Schimmelpfennig, B.; Maron, L.; Teichteil, C.; Leininger, T.; Gropen, O.; Grenthe, I.; Wahlgren, U. *Chem. Phys.* **1999**, *244*, 185.

(13) Vallet, V.; Maron, L.; Schimmelpfennig, B.; Leininger, T.; Teichteil, C.; Gropen, O.; Grenthe, I.; Wahlgren, U. *J. Phys. Chem. A* **1999**, *103*, 9285.

(14) Dolg, M.; Fulde, P.; Stoll, H.; Preuss, H.; Chang, A.; Pitzer, R. M. *Chem. Phys.* **1995**, *195*, 71.

(15) Maron, L.; Leininger, T.; Schimmelpfennig, B.; Vallet, V.; Heully, J.-L.; Teichteil, C.; Gropen, O.; Wahlgren, U. *Chem. Phys.* **1999**, *244*, 195.

(16) Wang, W.; Andrews, L.; Li, J.; Bursten, B. E. *Angew. Chem., Int. Ed.* **2004**, *43*, 2554. Ismail, N.; Heully, J.-L.; Saue, T.; Daudey, J.-P.; Marsden, C. J. *Chem. Phys. Lett.* **1999**, *300*, 296.

(17) See for instance: van Besien, E.; Pierloot, K.; Gorlier-Walrand, C. *Phys. Chem. Chem. Phys.* **2006**, 4311. Denning, R. G.; Green, J. C.; Hutchings, T. E.; Dallera, C.; Tagliaferri, A.; Giarda, K.; Brookes, N. B.; Braicovich, L. J. *J. Chem. Phys.* **2002**, *117*, 8008. Szabo, Z.; Toraishi, T.; Valet, V.; Grenthe, I. *Coord. Chem. Rev.* **2006**, *250*, 784.

(18) Belkiri, L.; Lissillour, R.; Boucekkine, A. *J. Mol. Struct. (THEOCHEM)* **2005**, *757*, 155. Hayton, T. W.; Boncella, J. M.; Scott, B. L. Palmer, P. D.; Batista, E. R.; Hay. P. J. *Science* **2005**, *310*, 1941. Hayton, T. W.; Boncella, J. M.; Scott, B. L.; Batista, E. R.; Hay, P. J. *J. Am. Chem. Soc.* **2006**, *128*, 10549.

(19) Maron, L.; Werkema, E. L.; Perrin, L.; Eisenstein, O.; Andersen, R. A. *J. Am. Chem. Soc.* **2005**, *127*, 279. Werkema, E. L.; Messines, E.; Perrin, L.; Maron, L.; Eisenstein, O.; Andersen, R. A. *J. Am. Chem. Soc.* **2005**, *127*, 7781. Sherer, E. C.; Cramer, C. J. *Organometallics* **2003**, *22*, 1682. Perrin, L.; Maron, L.; Eisenstein O. *New J. Chem.* **2004**, *10*, 1255. Barros, N.; Eisenstein, O.; Maron, L. *Dalton Trans.* **2006**, 3052.

(20) Zachmanoglou, C. E.; Docrat, A.; Bridgewater, B. M.; Parkin, G.; Brandow, C. G.; Bercaw, J. E.; Jardine, C. N.; Lyall, M.; Green, J. C.; Keister, J. B. *J. Am. Chem. Soc.* **2002**, *124*, 9525. Conejo, M. D.; Parry, J. S.; Carmona, E.; Schultz, M.; Brennan, J. G.; Beshouri, S. M.; Andersen, R. A.; Rogers, R. D.; Coles, S.; Hursthouse, M. *Chem.−Eur. J.* **1999**, *5*, 3000.

(21) Kanellakopoulos, B. In *Organometallics of the f Elements*; Marks, T. J., Fisher, R. D., Eds.; D. Riedel: Dortrecht, Holland, 1978; pp 1−36. Lukens, W. W.; Beshouri, S. M.; Blosch, L. L. Stuart, A. L.; Andersen R. A. *Organometallics* **1999**, *18*, 1235.

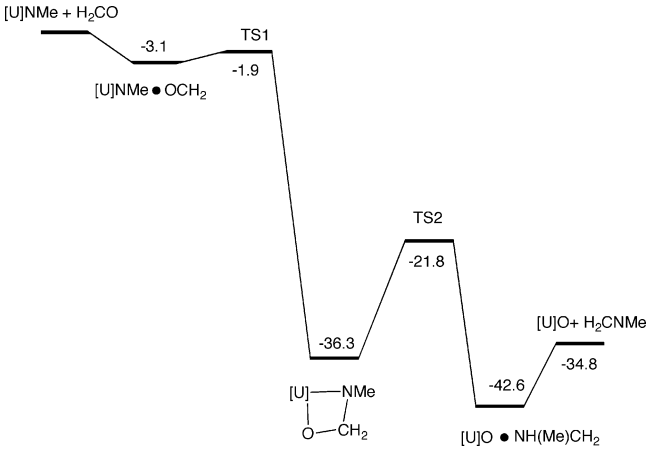

Figure 1. Free energy profile (ΔG, kcal mol^{-1}) for the reaction of Cp_2UNMe with $H_2C{=}O$ to form Cp_2UO and $H_2C{=}NMe$, [U] = Cp_2U.

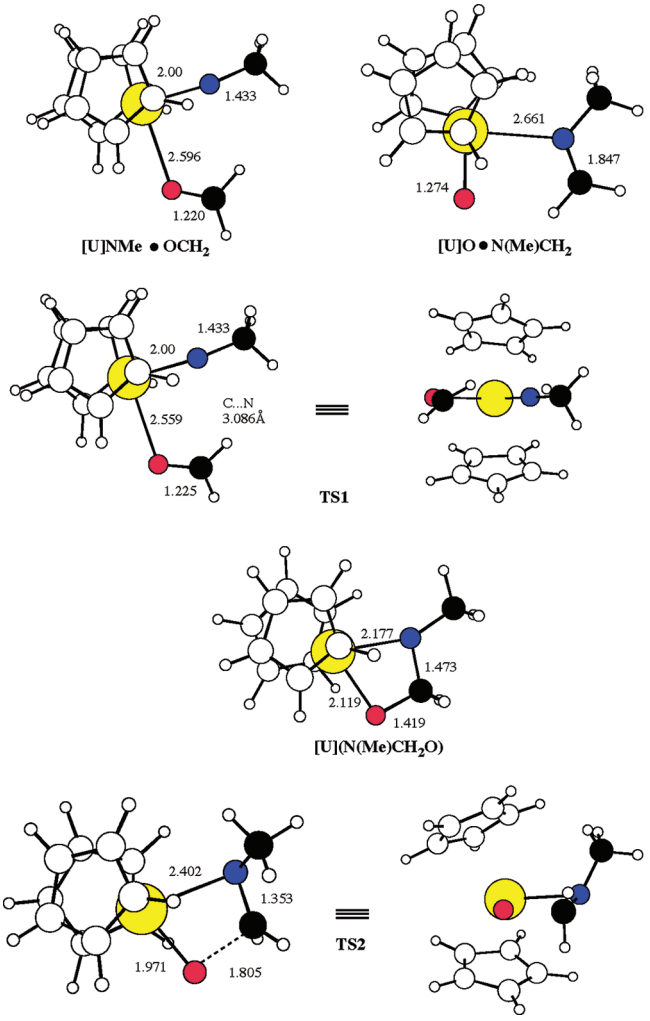

Figure 2. Optimized geometries (distance in Å, angle in deg) for the intermediates and transition states for the reaction of Cp_2UNMe with $H_2C{=}O$ to form Cp_2UO and $H_2C{=}NMe$. Two views of the transition states TS1 and TS2 are shown. Black circles are used for the carbon atoms in H_2CO and NMe, a red circle is used for oxygen, a blue circle is used for nitrogen, a yellow circle is used for uranium, and white circles are used for the carbon and the hydrogen atoms of the cyclopentadienyl ligand.

ligand in the experiments, which is replaced by C_5H_5 in the calculations. The experimental exchange reaction is general, since the arylimido derivatives $Cp'_2UN(4\text{-}(MeO)C_6H_4)$ and $Cp'_2UN(4\text{-}(Me_2N)C_6H_4)$ exchange rapidly with Ph_2CO; see Experimental Section for details.

$$Cp_2UNR + Ph_2C{=}O \rightarrow Cp_2UO + Ph_2C{=}NR \quad (R = Me \text{ or aryl}) \quad (1)$$

The reaction illustrated in eq 1 defines the free energy change and therefore the relative bond dissociation enthalpies of the reactants and products. The calculated ΔG and ΔH for eq 1, R = Me, are -26 and -28 kcal mol^{-1}, respectively, and the latter is close to the experimental value estimated for the difference between a C=O and a C=NR bond enthalpy.[3,22] In order to calculate the bond dissociation enthalpy of UO relative to UNMe, the free energy for dissociation of $Ph_2C{=}O$ into Ph_2C and O (both in their triplet ground states) and $Ph_2C{=}NMe$ into Ph_2C and NMe (both in their triplet ground states) is calculated, resulting in a bond dissociation enthalphy for $Ph_2C{=}O$ and $Ph_2C{=}NMe$ of 163 and 121 kcal mol^{-1}, respectively. This results in a UO bond dissociation enthalpy that is 70 kcal mol^{-1} greater than that of UNMe.[23]

The potential energy surface for the reaction symbolized in eq 1 is calculated for the reaction in which $Ph_2C{=}O$ and $Ph_2C{=}NMe$ are replaced by $H_2C{=}O$ and $H_2C{=}NMe$, respectively. Figure 1 shows the free energy profile, and Figure 2 shows the structures of the extrema. Figure 1 shows that the reaction is exoergic, since $\Delta G = -34.8$ kcal mol^{-1}, and irreversible. The reaction pathway proceeds by way of adduct formation, $[U]NMe{\cdot}OCH_2$, between the two reactants, where [U] is used as a symbol for Cp_2U. In this adduct, the formaldehyde molecule and the NMe fragment are coplanar; rotation of the CH_2 group around the O−C bond by 40°, so that the p orbital of CH_2 points toward nitrogen, yields the transition state that is only 1.2 kcal mol^{-1} above the adduct. The transition state TS1 connects to a four-center intermediate, which is 36.3 kcal mol^{-1} more stable than the separated reactants. The intermediate evolves by crossing a transition state TS2, which is 14.5 kcal mol^{-1} above the intermediate. In TS2, the π orbital of the $H_2C{=}NMe$ molecule and the U−O fragment are orientated so that the planes defined by the CH_2 and NUO atoms intersect at an angle of 139°. The transition state TS2 connects to an adduct between $H_2C{=}NMe$ and Cp_2UO, $[U]O{\cdot}N(Me)CH_2$, which is 42 kcal mol^{-1} below the separated reactants. In $[U]O{\cdot}N(Me)CH_2$, UO and $N(Me)CH_2$ are also coplanar so that the π orbital of the C=N bond is orthogonal to the UO bond. The free energy of the separated products Cp_2UO and $H_2C{=}NMe$ is higher than $[U]O{\cdot}N(Me)CH_2$ by about 10 kcal mol^{-1}, in accord with isolation of pyridine adducts in the experimental study.[1] The net reactions are cycloadditions followed by cycloreversions; in the cycloaddition transition state the π orbital of H_2CO is coplanar with the U−NMe bond, and in the cycloreversion transition state the π orbital of H_2CNMe also is coplanar with the U−O bond. In the adducts, $[U]NMe{\cdot}OCH_2$ and $[U]O{\cdot}N(Me)CH_2$, the π orbitals of the organic molecules are orientated away from the uranium fragment. Thus, the free activation energies of these elementary steps are relatively low since they are associated with bond rotations that do not require significant electronic reorganization.

The net metathesis of an oxygen atom for a NMe group is exoergic because the UO bond is stronger than that of UNMe. The relatively low activation energies of the two elementary steps calculated for the reaction illustrated in eq 1, in which Ph_2CO is replaced by H_2CO, are consistent with the rapid reaction observed in the experimental exchange reaction in which no intermediates are observed in the ^{1}H NMR spectrum.

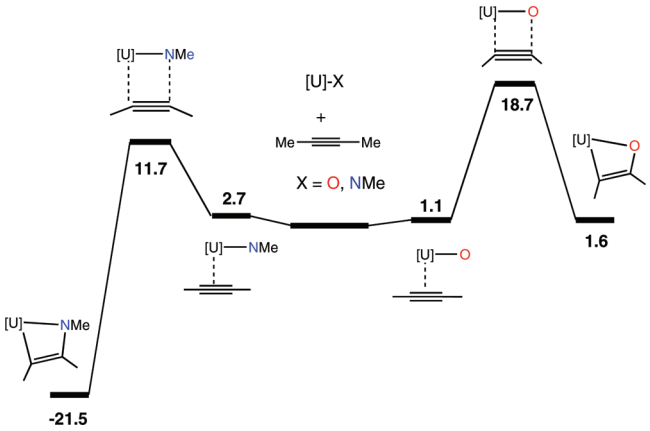

Figure 3. Free energy profile (ΔG in kcal mol^{-1}) for the 1,2-cycloaddition of dimethylacetylene to (a, left-hand side) Cp_2UNMe and (b, right-hand side) Cp_2UO, [U] = Cp_2U.

Reaction of Cp_2UO and Cp_2UNMe with MeC≡CMe. The calculated free energy profiles for the reactions illustrated in eqs 2 and 3 are shown in Figure 3.

$$Cp_2UNMe + MeC{\equiv}CMe \rightarrow Cp_2UN(Me)C(Me){=}C(Me) \quad (2)$$

$$Cp_2UO + MeC{\equiv}CMe \rightarrow Cp_2UOC(Me){=}C(Me) \quad (3)$$

The left-hand side of Figure 3 shows that the transformation in eq 2 is thermodynamically favorable ($\Delta G = -21.5$ kcal mol^{-1}) and the activation energy is only 11.7 kcal mol^{-1} from the separated reactants. These calculated free energies are in agreement with the experimental reaction in which the azametallacycle is isolated and therefore exists as a minimum on the potential energy surface. In solution, the azametallacyle, $Cp'_2UN(Me)C(Me){=}C(Me)$, does not exchange, on the NMR time scale, with added dimethylacetylene or other substituted alkynes, showing that the reaction in eq 2 is not reversible, consistent with the calculated values shown in Figure 3. Thus, the reaction between Cp_2UNMe and MeC≡CMe gives a stable azametallacycle, whose structure, shown in Figure 4, closely resembles that of the isolated metallacyle,[2] which in turn resembles the intermediate in the metathesis reaction illustrated in eq 1.

The calculated free energy profile for formation of an oxametallacyclobutane, shown in eq 3, is illustrated on the right-hand side of Figure 3. The optimized geometries of all extrema are shown in Figure S1 of the Supporting Information. The calculated free energy change is endoergic, consistent with the experimental result that dimethylacetylene does not react with the oxouranium metallocene even though the activation energy is less than that for the formation of the azametallacyclobutane. This clear-cut result is due to the thermodynamic stability of the UO bond relative to that of the UNMe bond.

Reaction of Cp_2UO and Cp_2UNMe with H_3SiX (X = Cl, H). The calculated free energy profiles for the reaction of Cp_2UO and Cp_2UNMe with H_3SiCl is shown in Figure 5. The optimized geometries of all extrema are shown in Figures S2 and S3 of the Supporting Information. The calculated reaction coordinate shows that both reactions are exoergic by about −30 kcal mol^{-1}. The activation energies for both reactions are low, and the reactions are essentially barrierless. The computational results are surprising since the experimental result is that Me_3SiCl reacts slowly with Cp'_2UO but does not react with either Cp'_2UNMe or $Cp'_2UN(4\text{-}MeC_6H_4)$. It seems reasonable to suggest that the model calculation in which 1,2,4-$(CMe_3)_3C_5H_2$ is replaced by C_5H_5 and Me_3Si by H_3Si greatly underestimates the steric effects involved in the transition state; that is, as Me_3SiCl approaches the U−NMe fragment, the U−N−Me angle changes from 180° to about 120° as the N−$SiMe_3$ bond develops. This motion moves the NMe group into the wedge of the $[\eta^5\text{-}1,2,4\text{-}(CMe_3)_3C_5H_2]_2U$ fragment, resulting in a transition state whose energy is much higher in the experimental system than in the calculated one.

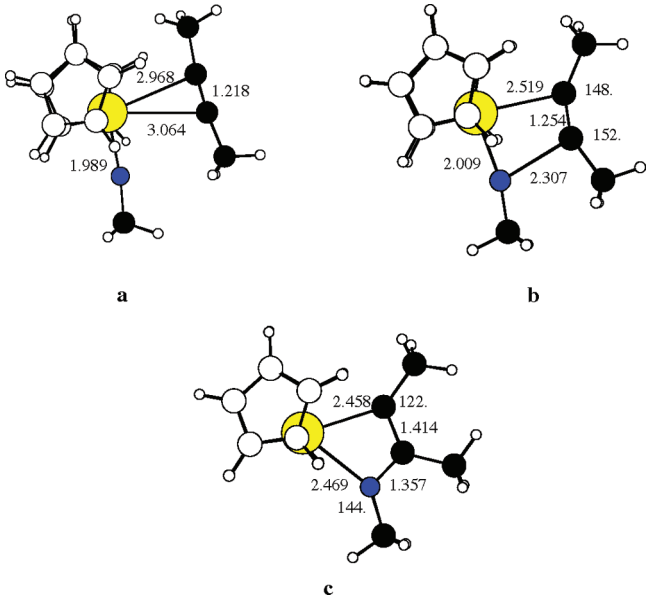

Figure 4. Optimized structures of (a) the adduct [U]NMe·(MeC≡CMe), (b) the transition state for the cycloaddition, and (c) the azametallacyclobutene in Figure 3. The color code for the atoms is identical to that used in Figure 2.

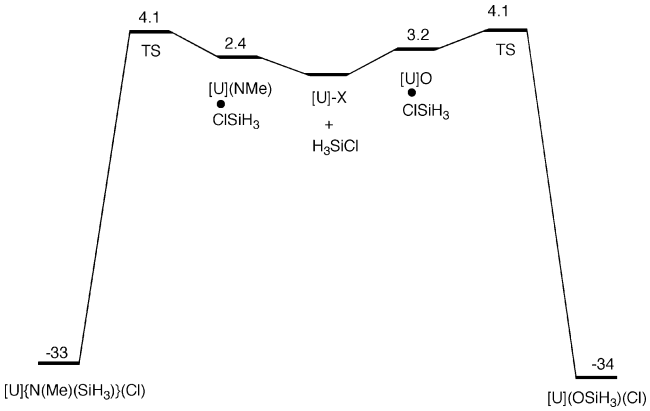

Figure 5. Free energy profile (ΔG in kcal mol^{-1}) for the 1,2-addition of H_3SiCl to (a, left-hand side) Cp_2UNMe and (b, right-hand side) Cp_2UO, [U] = Cp_2U.

The calculated free energy profiles for the reaction of SiH_4 with either Cp_2UO or Cp_2UNMe (Figures S4 and S5 in the Supporting Information show the geometries of the extrema) show that both reactions are endoergic, since a UH bond is weaker than a UCl bond.[24] Although the reaction with SiH_4 is not studied experimentally, the reaction of the dihydrogen, which is a useful model for SiH_4, does not react with either metallocene derivative.In summary, all of the calculated potential energy surfaces for these metathesis and addition reactions show that

(22) Sandorfy, C. In *The Chemistry of the C-N Double Bond*; Patai, S., Ed.; Interscience: London, 1970; Chapter 1.

(23) ΔH(reaction) for eq 1 = {Cp_2U}{O} + {Ph_2C}{NMe} − ({Cp_2U}{NMe} + {Ph_2C}{O}) where the brackets indicate the chemical fragments involved in the calculation of the bond dissociation energies. Replacing ΔH(reaction), {Ph_2C}{NMe}, and {Ph_2C}{O} by the values −28, 121, and 163 kcal mol^{-1}, respectively, yields the difference {U}{O} − ({U}{NMe}) = 70 kcal mol^{-1}.

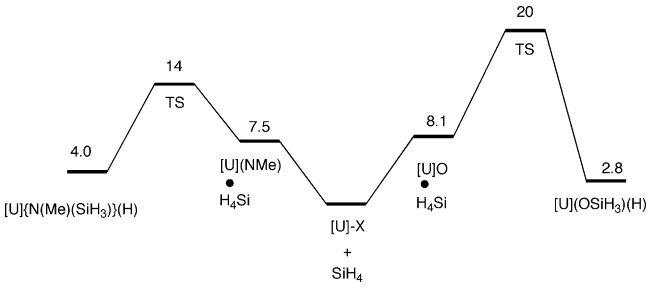

Figure 6. Free energy profile (ΔG in kcal mol^{-1}) for the 1,2-addition of H_4Si to (a, left-hand side) Cp_2UNMe and (b, right-hand side) Cp_2UO, [U] = Cp_2U.

they are under thermodynamic control. Thus, the change in free energy between the initial and final states determines the net chemical reaction, and the strength of the UO and UNMe bonds plays the controlling role. A corollary is that a bond model that describes the ground-state electronic structures is essential in order to understand the reactions at the molecular level; a model is described below.

Calculated Molecular and Electronic Structure of Cp_2UX (X = O, NMe) and Validation of the DFT Calculations. Cp_2UO. DFT calculations show that the ground-state configuration is a triplet and the two unpaired electrons reside in two 5f orbitals. The first singlet state is calculated to be 39 kcal mol^{-1} higher in energy at this level of calculation. The DFT-optimized geometry of Cp_2UO in the triplet state is shown as [U]O in Figure 2. The calculated structure can be compared only to that of the 4-dimethylaminopyridine adduct, Cp'_2UO-(4-(Me_2N)pyridine), because the structure of base-free Cp'_2UO is unknown. The calculated UO distance of 1.829 Å is close to the experimental value of 1.860(3) Å, and the average U−C(Cp) distance of 2.80 Å compares well with the experimental value of 2.87 Å. The Cp−U−Cp angle of 121° is significantly smaller than the experimental value of 142°, which is expected since C_5H_5 is sterically smaller than the 1,2,4-tri-*tert*-butylcyclopentadienyl ligands in the experimental system. The calculated, unscaled, UO stretching frequency of 811 cm^{-1} is in reasonable agreement with the experimental value of 760 cm^{-1} found for the pyridine adduct. Thus, the DFT calculation on the model base-free complex, Cp_2UO, reproduces the main geometrical features found in $Cp'_2UO(L)$. The agreement between the calculated and experimental UO stretching frequencies suggests that the shape of the potential energy surface for the UO bond is not influenced greatly by the presence of the Lewis base and that the UO stretching motion is not strongly coupled to the other stretching motions.

The NBO analysis on Cp_2UO shows that the uranium and oxygen atoms carry charges of +2.49 on uranium and −1.11 on oxygen; therefore the charge on the Cp_2U fragment is +1.11, and each Cp ring carries a charge of −0.7. The charge on U is rather large but significantly smaller than the value implied by the oxidation number. This is in contrast to the charge in, for example, Cp_2CeF or Cp_2CeOMe, where the charge on Ce is closer to the oxidation number. The lower NBO charge to oxidation number ratio (0.62) in Cp_2UO relative to that found in Cp_2CeF or Cp_2CeOMe (0.85) corresponds to the traditional view that the bonding in actinide metal compounds utilizes the 5f electrons, whereas the 4f electrons in the lanthanide metals are essentially core electrons and are little used in 4f metal to ligand bonds.[25] These two bonding types are usually described by the vague and imprecise terms "covalent" and "ionic" bonding that may be quantitatively expressed by the NBO/oxidation number ratio; the lower the ratio, the more covalent the bond due to greater sharing of electrons, i.e., covalence.

In Cp_2UO, the NBO charges show that the U−O bond is a σ bond constructed from 80% of the oxygen atom (95% p + 5% s) and 20% from a uranium hybrid orbital largely made from 5f orbitals with a small contribution (8%) from the 6d orbitals. The σ bond is strongly polarized toward the oxygen atom, and the other six electrons on oxygen are nonbonding lone pairs, one along and two perpendicular to the U−O axis. The donor−acceptor interaction between the oxygen lone pairs and the uranium fragment is small since a second-order perturbation analysis of the bonding shows that the three lone pairs transfer a total of only 0.2 electron to uranium. Therefore, the interaction between U and O is a single U−O σ bond polarized toward oxygen and the U−O bond enthalpy results mainly from Coulombic attraction between the oppositely charged atoms over a short distance augmented by a small orbital contribution, resulting in a small amount of covalence in the bond. This bond model supports the view that the resonance structure $Cp_2U^{(+)}$−$O^{(-)}$ dominates Cp_2U═O.

A multiconfigurational, localized-orbital calculation on the DFT-optimized geometry supports the model of the U−O bond derived from the DFT calculations. A CAS(2,7) distributing two electrons among the seven 5f orbitals has been carried out. It confirms the triplet nature of the ground state with two unpaired electrons and more importantly shows that this state is properly described by a single reference configuration (85%) with a contribution of only 15% from another configuration. These two configurations differ only by the angular momentum quantum numbers of the nondegenerate 5f orbitals in which the two electrons reside. The localized orbitals show the presence of three lone pairs on oxygen and a σ bond between Cp_2U and O. Furthermore, a geometry optimization at the CASSCF level gives a geometry similar to that obtained from the DFT calculations. These results, therefore, validate the use of DFT methodology for Cp_2UO.

Cp_2UNMe. The calculated geometrical parameters are in satisfactory agreement with those obtained for Cp'_2U(N-4-MeC_6H_4), since the crystal structure of Cp'_2UNMe is unknown. The calculated U−N distance of 1.982 Å agrees with the experimental value of 1.988(5) Å, and the calculated U−N−C(Me) angle of 180° agrees with the experimental value for U−N−C(4-MeC_6H_4) of 172.3(5)°.

An NBO analysis gives a charge of +2.38 on U, −0.70 on Cp so that the total negative charge on Cp_2U is +0.99, −1.15 on N, and +0.16 on the methyl group, resulting in the total negative charge on the nitrene fragment of −0.99. The NBO charge to oxidation number ratio in the NMe metallocene of 0.60 implies that the UNMe bond is slightly more covalent than the U−O bond, where the ratio is 0.62. This deduction is supported by the NBO analysis, which shows the presence of σ and π bonds; the σ bond is built from 51% of the nitrogen p orbital and 49% of the uranium 5f (97%) and 6d (3%) orbitals. The π bond, which is built from 80% of the nitrogen p orbital and 20% of the uranium 5f (78%) and 6d (22%) orbitals, is polarized toward nitrogen. In addition, the second-order perturbation term shows that the lone pair located on nitrogen has

(24) Bruno, J. W.; Stecher, H. A.; Morss, L. R.; Sonnenberger, D. C.; Marks, T. J. *J. Am. Chem. Soc.* **1986**, *108*, 7275. Jemine, X.; Goffart, J.; Berthet, J. C.; Ephritikhine, M. *J. Chem. Soc., Dalton Trans.* **1992**, 2439. Leal, J. P.; Marques, N.; Pires de Matos, A.; Calhorda, M. J.; Galvao, A. M.; Martinho Simoes, J. A. *Organometallics* **1992**, *11*, 1632. Martinho Simoes, J. A.; Leal, J. P. *ChemTracks Inorg. Chem.* **1991**, *3*, 143. Leal, J. P.; Marques, N.; Takats J. *J. Organomet. Chem.* **2001**, *632*, 209.

(25) (a) The first indication of covalency in the 5f-block metals was the observation of ^{19}F superhyperfine splitting in the EPR spectrum of U(III) atoms in CaF_2. Bleany, B.; Llewellyn, P. M.; Jones, D. A. *Proc. Phys. Soc.* **1956**, *B69*, 858. (b) Maron, L.; Eisenstein, O. *J. Phys. Chem. A* **2000**, *104*, 7140.

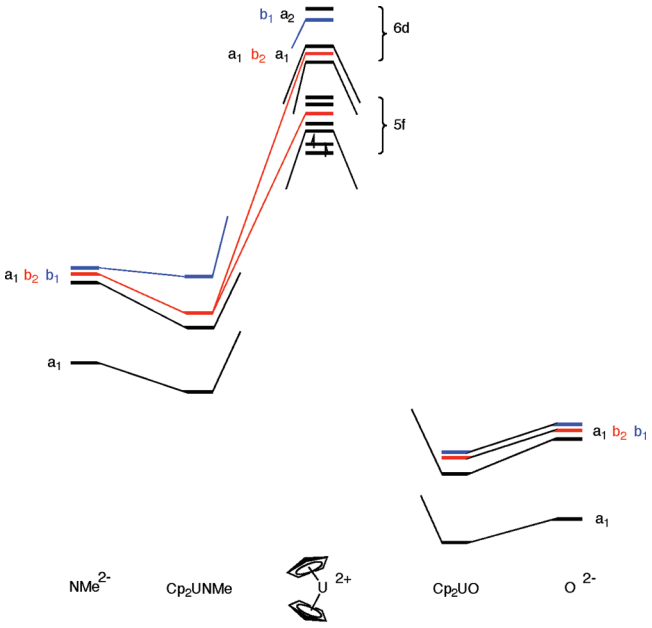

Figure 7. Schematic representation of the fragment molecular orbitals of [U], O, and NMe, which combine to form [U]O and [U]NMe in C_{2v} symmetry. Only the metal-centered orbitals are shown and the NMe and O orbitals are doubly occupied. The low symmetry of the molecules results in metal-centered orbitals of mixed parentage, and graphic representations of these orbitals are not shown. The absence of correlation lines to the b_1 and b_2 oxygen orbitals indicates that they are nonbonding lone pairs.

62% s and 38% p character, a hybridization that is different from that used by nitrogen to build the U−N double bond, and the lone pair interacts with an empty orbital on uranium made from 7s, 6d, and 5f contributions; this delocalization accounts for the linear UNMe geometry.

The multiconfigurational, localized-orbital calculation on the geometry optimized from the DFT calculations gives a triplet electronic ground state as found in Cp_2UO. The triplet ground state is also a combination of two determinants (85% and 15%) as found in Cp_2UO. Furthermore, the geometry optimization at the CASSCF level gives a geometry identical to that obtained at the DFT level. The localized orbitals show a UN double bond and a lone pair on the NMe group, which interacts with the Cp_2U fragment. Thus, the bonding picture for the imidometallocenes derived from the DFT agrees with the multiconfigurational calculations, which again validates the use of DFT calculations for Cp_2UNMe.

The demonstrated applicability of the DFT calculations for the molecules described in this article raises and answers the question of the general application of the DFT methodology in open-shell systems. In the molecules studied here, the low symmetry and the low ligand field remove the degeneracy of the 5f orbitals to yield one dominating configuration, which justifies the use of DFT methodology.

Comparison of the Bonding in Cp_2UO and Cp_2UNMe. Although the NBO charges on the Cp_2U fragments in these two metallocene derivatives are similar, the nature of their chemical bonds to the oxygen and nitrene fragments is different, resulting in the UNMe bond being thermodynamically weaker than the UO bond. In molecular orbital language, the UO bond in Cp_2UO may be formulated by combining the $Cp_2U^{(2+)}$ and $O^{(2-)}$ fragments as shown in Figure 7. The U−O bond is largely oxygen in character and the electrons in the p_x and p_y orbitals are largely nonbonding. The molecular orbital description of the UNMe bond is rather different since the orbitals on the $NMe^{(2-)}$ fragment are closer in energy to those of the $Cp_2U^{(2+)}$ fragment orbitals; the experimental electron affinity of O is 1.46 eV while that of NMe is 0.02 eV,[8] resulting in a UNMe bond that is more covalent.

The bonding in the four-membered-ring metallacycles formed from the addition of dimethylacetylene to [U]O or [U]NMe has no remarkable features. The [U]−O and [U]−N bonds are longer than in the corresponding reactants, which weakens them; a similar comment applies to [U](Cl)($OSiH_3$) and [U](Cl){N(Me)-(SiH_3)}.

Origin of the Reactivity Difference between Cp_2UO and Cp_2UNMe. The reaction of Cp_2UO and Cp_2UNMe with dimethylacetylene is the 1,2-addition of a polar U−X bond, in each case, to a nonpolar triple bond. The UO and UNMe bond can use more than one orbital in the cycloaddition; no symmetry restriction governs this process and the reaction cannot be considered forbidden, so that the activation energies are modest in each case. The difference in the net reactions, viz., Cp_2UNMe forms a cycloadduct and Cp_2UO does not, is associated with the net enthalpy changes. The bond analysis of Cp_2UO shows the presence of a single U−O bond with nonbonding lone pairs on oxygen. In contrast, the bond analysis of Cp_2UNMe shows the presence of a double UNMe bond and a lone pair on the NMe fragment. The calculated heat of reaction between Cp_2-UNMe and Ph_2CO to form Cp_2UO and Ph_2CNMe shows that the UO bond is stronger than the UNMe bond by about 70 kcal mol^{-1}. Therefore, it is not surprising that the UO bond is unreactive since it has to overcome this energy penalty.

The reaction of Cp_2UO or Cp_2UNMe with H_3SiCl is also a 1,2-addition reaction in which the Si−Cl bond adds to the UO or UNMe fragments. These net reactions are essentially barrierless and equally exoergic, a consequence of the formation of strong U−Cl, UO−Si, and UN−Si bonds. The thermochemistry of the 1,2-addition reactions is different from that of the cycloaddition reactions, although the two types of reactions proceed through metathesis-like transition states. The experimental outcome of the reaction of Me_3SiCl with Cp'_2UO or Cp'_2UNMe (Cp′ = 1,2,4-tri-*tert*-butylcyclopentadienyl) is however different from the calculational outcome, since although $Cp'_2U(OSiR_3)Cl$ forms and $Cp'_2UN(Me)(SiR_3)Cl$ does not, a result most reasonably ascribed to steric effects of the substituents on the imido group with those on the cyclopentadienyl rings. In the case of SiH_4, the calculations indicate that the reaction with Cp_2UO and Cp_2UNMe is endoergic, the result of the weaker UH bond relative to a UCl bond.

Summary

The calculated free energy profiles for the reaction of Cp_2UNMe with ketones and acetylenes and Cp_2UO with silylhalides show that the reactions are under thermodynamic control since the reactions proceed with modest activation free energies. The calculated results mirror the experimental results for $[1,2,4\text{-}(CMe_3)_3C_5H_2]_2UNMe$ with benzophenone and dimethylacetylene and for $[1,2,4\text{-}(CMe_3)_3C_5H_2]_2UO$ with Me_3SiCl. The origin of the reactivity differences is traced to the strength of the UO bond relative to that of the UNMe bond. The stronger UO bond is not a "double bond", but it is a strongly polarized one in which the dominant resonance structure is $Cp_2U^{(+)}-O^{(-)}$, presumably due to the large electronegativity of the oxygen atom. On the other hand, the thermodynamically weaker UNMe bond has more "double-bond" character, the net result of the lower electronegativity of the NMe group. Thus, these bonds display different reactivity patterns because of their different bond strengths, and these differences are not related

to their multiple-bond character. This conclusion, at first glance, is counterintuitive, because our intuition is developed from a pure covalent bond model in which bond order scales with bond strength. This inference fails when the electrostatic interactions dominate the orbital interactions, as in the molecules described herein.

Experimental Details

The experimental studies were carried out as previously described.[1,2] The reaction of Cp'_2UNMe, Cp'_2UO, or $Cp'_2UO(4\text{-}(Me_2N)C_6H_4)$ in the presence of BPh_3, with dihydrogen or dideuterium, was carried out in a sealed NMR tube at 1 atm total pressure in C_6D_6.

Reaction of $[\eta^5\text{-}1,2,4\text{-}(CMe_3)_3C_5H_2]_2UN(4\text{-}(MeO)C_6H_4)$ with Ph_2CO. NMR Scale. To an NMR tube charged with $[\eta^5\text{-}1,2,4\text{-}(CMe_3)_3C_5H_2]_2UN(4\text{-}(MeO)C_6H_4)$ (17 mg, 0.02 mmol) and C_6D_6 (0.5 mL) was added benzophenone (3.6 mg, 0.02 mmol). The color of the solution immediately changed from dark brown to brown-red. The ^{1}H NMR spectrum contained resonances due to $[\eta^5\text{-}1,2,4\text{-}(CMe_3)_3C_5H_2]_2UO$ and $Ph_2C{=}N\text{-}4\text{-}(MeO)C_6H_4$[26] (^{1}H NMR ($C_6D_6$): δ 7.94 (m, 2H, aryl *H*), 7.03−6.87 (m, 8H, aryl *H*), 6.74 (m, 1H, aryl *H*), 6.57 (m, 1H, aryl *H*), 6.37 (m, 2H, aryl *H*), 3.45 (s, 3H, CH_3)) (100% conversion relative to an internal standard).

Reaction of $[\eta^5\text{-}1,2,4\text{-}(CMe_3)_3C_5H_2]_2UN(4\text{-}(Me_2N)C_6H_4)$ with Ph_2CO. NMR Scale. To an NMR tube charged with $[\eta^5\text{-}1,2,4\text{-}(CMe_3)_3C_5H_2]_2UN(4\text{-}(Me_2N)C_6H_4)$ (18 mg, 0.02 mmol) and C_6D_6 (0.5 mL) was added benzophenone (3.6 mg, 0.02 mmol). The color of the solution immediately changed from dark brown to brown-red. The ^{1}H NMR spectrum contained resonances due to $[\eta^5\text{-}1,2,4\text{-}(CMe_3)_3C_5H_2]_2UO$ and $Ph_2C{=}N\text{-}4\text{-}(Me_2N)C_6H_4$[27] (^{1}H NMR ($C_6D_6$): δ 7.92 (m, 2H, aryl *H*), 6.97 (m, 6H, aryl *H*), 6.84 (m, 2H, aryl *H*), 6.71 (m, 1H, aryl *H*), 6.55 (m, 1H, aryl H), 6.37 (m, 2H, aryl *H*), 3.19 (s, 6H, CH_3)) (100% conversion relative to an internal standard).

Computational Details. The Stuttgart−Dresden−Bonn small-core relativistic effective core potential (RECP) has been used to represent the 78 core electrons of U, leaving 14 valence electrons in the 6s, 6p, 5f, 6d, and 7s shells.[28] The associated basis set, including up to g functions, has been used to represent the valence orbitals. C, N, O, and H have been represented by an all-electron 6-31G(d,p) basis set.[29] Si and Cl atoms were also treated with a large-core RECP in combination with the adapted basis set,[30] augmented by a polarization d function (Si, exp = 0.284), Cl exp = 0.643.[31] Calculations have been carried out at the DFT(B3PW91) level[32] with Gaussian 03.[33] The nature of the extrema (minimum or transition state) has been established with analytical frequency calculations, and the intrinsic reaction coordinate (IRC) has been followed to confirm that transition states connect to reactants and products. The zero-point energy (ZPE) and entropic contribution have been estimated within the harmonic potential approximation. The enthalpies ΔH and Gibbs free energy, ΔG, were calculated for $T = 298.15$ K and 1 atm (for ΔG). The population analysis was carried out using the NBO methodology.[34]

The validity of the DFT approach was determined by a wave function based method. The SCF calculations were carried out with the MOLCAS 6 suite of programs,[35] and the subsequent CASSCF calculations with localized orbitals were performed with the NOSCF program.[36] In these calculations the U atom was treated with an *ab initio* model potential (AIMP)[37] including 78 electrons in the core with the associated basis sets. The C, N O, and H atoms were represented with ANO-type basis sets.[38] The CASSCF(2,7) calculations, carried out on the DFT-optimized geometry, revealed that two configurations had to be considered. Consequently the geometry optimization at the CAS level was carried out for a CASSCF(2,2) for selected cases.

Acknowledgment. This work was partially supported by the Director of Energy Research Office of Basic Energy Sciences, Chemical Sciences Division of the U.S. Department of Energy, under Contract No. DE-AC02-05CH11231. Calculations were in part carried out at the national computing centers CINES and CALMIP (France). N.B. thanks the Commissariat à l'Energie Atomique (CEA), France, for funding. O.E. thanks the Miller Institute for a Visiting Miller Professorship at U.C. Berkeley. The French authors thank the CNRS, notably the PICS 3422, and the Ministère of National Education for funding.

Note Added after ASAP Publication: In the version published on Sept 1, 2007, refs 26−32 were misnumbered. The corrected version was posted on Sept 5, 2007.

Supporting Information Available: Optimized geometries of the intermediates and transition states for the reactions of Cp_2UO and $MeC{\equiv}CMe$ (Figure S1), Cp_2UO and H_3SiCl (Figure S2), Cp_2UMe and H_3SiCl (Figure S3), Cp_2UO and SiH_4 (Figure S4), and Cp_2UMe and SiH_4 (Figure S5). List of coordinates, energy and free energy of all optimized species. This material is available free of charge via the Internet at http://pubs.acs.org.

OM700628E

(26) Okubo, M.; Ueda, S. *Bull. Chem. Soc. Jpn.* **1980**, *53*, 281.
(27) Henderson, W. A.; Zweig, A. *Tetrahedron* **1971**, *27*, 5307.
(28) http://www.theochem.uni-stuttgart.de/pseudopotentiale/clickpse.en.html.
(29) Hariharan, P. C.; Pople, J. A. *Theor. Chim. Acta* **1973**, *28*, 213.
(30) Bergner, A.; Dolg, M.; Kuchle, W.; Stoll, H.; Preuss, H. *Mol. Phys.* **1993**, *80*, 1431.
(31) Maron, L.; Teichteil, C. *Chem. Phys.* **1998**, *237*, 105.
(32) Perdew, J. P.; Wang, Y. *Phys. Rev. B* **1992**, *45*, 13244. Becke, A. D. *J. Chem. Phys.* **1993**, *98*, 5648. Burke, K.; Perdew, J. P.; Yang, W. In *Electronic Density Functional Theory: Recent Progress and New Directions*; Dobson, J. F., Vignale, G., Das, M. P., Eds.; Plenum: New York, 1998.
(33) Frisch, M. J.; Trucks, G. W.; Schlegel, H. B.; Scuseria, G. E.; Robb, M. A.; Cheeseman, J. R.; Montgomery, J. A.; Vreven, T.; Kudin, K. N.; Burant, J. C.; Millam, J. M.; Iyengar, S. S.; Tomasi, J.; Barone, V.; Mennucci, B.; Cossi, M.; Scalmani, G.; Rega, N.; Petersson, G. A.; Nakatsuji, H.; Hada, M.; Ehara, M.; Toyota, K.; Fukuda, R.; Hasegawa, J.; Ishida, M.; Nakajima, T.; Honda, Y.; Kitao, O.; Nakai, H.; Klene, M.; Li, X.; Knox, J. E.; Hratchian, H. P.; Cross, J. B.; Bakken, V.; Adamo, C.; Jaramillo, J.; Gomperts, R.; Stratmann, R. E.; Yazyev, O.; Austin, A. J.; Cammi, R.; Pomelli, C.; Ochterski, J. W.; Ayala, P. Y.; Morokuma, K.; Voth, G. A.; Salvador, P.; Dannenberg, J. J.; Zakrzewski, V. G.; Dapprich, S.; Daniels, A. D.; Strain, M. C.; Farkas, O.; Malick, D. K.; Rabuck, A. D.; Raghavachari, K.; Foresman, J. B.; Ortiz, J. V.; Cui, Q.; Baboul, A. G.; Clifford, S.; Cioslowski, J.; Stefanov, B. B.; Liu, G.; Liashenko, A.; Piskorz, P.; Komaromi, I.; Martin, R. L.; Fox, D. J.; Keith, T.; Al-Laham, M. A.; Peng, C. Y.; Nanayakkara, A.; Challacombe, M.; Gill, P. M. W.; Johnson, B.; Chen, W.; Wong, M. W.; Gonzalez, C.; Pople, J. A., Jr. *Gaussian 03*, Revision C.02; Gaussian, Inc.: Wallingford, CT, 2004.
(34) Reed, A. E.; Curtiss, L. A.; Weinhold, F. *Chem. Rev.* **1988**, *88*, 899.
(35) Karlström, G.; Lindh, R.; Malmqvist, P.-Å.; Roos, B. O.; Ryde, U.; Veryazov, V.; Widmark, P.-O.; Cossi, M.; Schimmelpfennig, B.; Neogrady, P.; Seijo, L. *Comput. Mater. Sci.* **2003**, *28*, 222, <http://www.teokem.lu.se/molcas/documentation/manual/node85.html#Karlstroem:03a>.
(36) Maynau, D.; Evangelisti, S.; Guihery, N.; Calzado, C. J.; Malrieu, J.-P. *J. Chem. Phys.* **2002**, *116*, 10060.
(37) Seijo, L.; Barandiaran, Z.; Harguindey, E. *J. Chem. Phys.* **2001**, *114*, 118.
(38) Widmark, P.-O.; Malmqvist, P.-A.; Roos, B. O. *Theor. Chim. Acta* **1990**, *77*, 291.